

## Time-Resolved Dual-Beam Two-Photon Interferences with High Visibility

J. Brendel, E. Mohler, and W. Martienssen

*Physikalisches Institut der Universität Frankfurt am Main, D-6000 Frankfurt am Main, Federal Republic of Germany*

(Received 5 November 1990)

We perform a two-photon interference experiment in a Michelson interferometer with photon pairs produced by spontaneous parametric down-conversion. The interferometer is set to a path difference much larger than the coherence length of the light field. Application of a time-resolved coincidence detection scheme reveals two-photon interference fringes with a visibility of 87%. This high visibility clearly demonstrates the nonclassical nature of the observed interference and should allow further spin-free tests of Bell's inequalities.

PACS numbers: 42.50.-p, 07.60.Ly

During the last years a number of experiments using correlated photons in a pair state have been performed to demonstrate fourth-order interference effects. These manifest themselves as a phase-dependent variation of the photon correlation in the detected light field, and they can be obtained even in the absence of the familiar second-order or intensity interferences. Fourth-order interferences were first observed in experiments regarding the correlation of spatially separated photons of a pair.<sup>1-4</sup>

A related interference effect has been demonstrated recently using Michelson interferometers driven by photon pairs.<sup>5,6</sup> Although the path difference between the arms of the interferometer exceeded the coherence length of the light by far, correlation measurements between the interferometer outputs still exhibited interference fringes with visibilities close to a value of 50%. In these experiments, the observed correlation interference can be understood as the interference of photon pairs with themselves. However, one has to take into consideration that part of the photon pairs are split during passing the interferometer. For large path differences and low temporal resolution these processes result in an unmodulated background in the interference thus limiting the visibility to 50%.

It has been pointed out that fourth-order interferences with visibilities up to 50% in the absence of second-order interferences could also be obtained with classical light fields.<sup>5,7-10</sup> On the other hand, the possibility of such an explanation has been questioned.<sup>6</sup> In any case, if visibilities above 50% are obtained, they unambiguously demonstrate the nonclassical nature of the pair state.

Fourth-order interferences can also be used for spin-free tests of Bell's inequalities.<sup>11,12</sup> In particular, interferences in large-path-difference interferometers have been suggested for such a test.<sup>13,14</sup> Experiments of this type, however, would require visibilities exceeding a value of  $(\frac{1}{2})^{1/2} = 71\%$ . Therefore it appears promising to improve the experiments with Michelson interferometers aiming at visibilities larger than those obtained up to now.

In this Letter, we report on an experiment which allows one to eliminate the background of split photon pairs in the interferogram. This elimination is achieved by highly time-resolved coincidence detection; it leads to fourth-order interferences with visibilities much larger than 50% and also larger than the Bell limit of 71%. The path differences exceed the coherence length by orders of magnitude.

The photon pairs are produced by spontaneous parametric down-conversion. The process, in which the photons of a pair are emitted simultaneously,<sup>15,16</sup> obeys the frequency and (inside the crystal) wave-vector conservation relations

$$\omega_p = \omega_s + \omega_i, \quad \mathbf{k}_p = \mathbf{k}_s + \mathbf{k}_i. \quad (1)$$

Here  $\omega_p$  and  $\mathbf{k}_p$  denote the frequency and the wave vector of the pump photons, respectively, and  $\omega_s, \omega_i, \mathbf{k}_s, \mathbf{k}_i$  are the corresponding quantities for the created signal and idler photons. The transmission probability  $P_{22}(\delta)$  for photon pairs in a Michelson interferometer can be derived by regarding the four different ways the pair can traverse the interferometer from the entrance arm to the exit arm (see Fig. 1). Representing each quantum-mechanical process by a complex probability amplitude,<sup>17,18</sup> the total probability is given by

$$P_{22}(\delta) = \langle R^2 T^2 | 1 + \exp[i(\delta + \delta_{rs})] + \exp[i(\delta + \delta_{ri})] + \exp[i(2\delta + \delta_{rs} + \delta_{ri})] |^2 \rangle, \quad (2)$$

where the terms 1-4 of the sum correspond to the

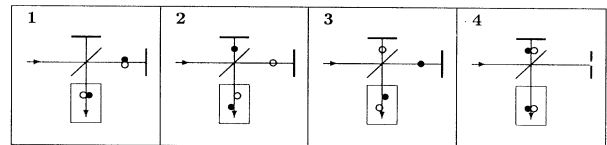


FIG. 1. Possible processes of photon-pair propagation inside a Michelson interferometer. The small boxes schematically indicate "snapshots" of those pairs where both photons are leaving the interferometer through the exit arm.

transmission paths 1–4 shown in Fig. 1. Here,  $\delta$  is the phase difference between the interfering beams for coherent light and  $\delta_{rs}$  and  $\delta_{ri}$  are random deviations of the phase differences due to the frequency distributions within the signal and idler beams. Because of the constraints, Eq. (1), the random deviations obey the relation  $\delta_{rs} + \delta_{ri} = 0$ .  $R$  and  $T$  are the reflectivity and the transmissivity of the interferometer beam splitter, respectively, and the brackets  $\langle \rangle$  denote averages over the random fluctuations  $\delta_{rs}$  and  $\delta_{ri}$ .

We will now assume that the path difference is much larger than the coherence length of signal and idler photons, but still smaller than the coherence length of the pump light. The random phase differences  $\delta_{rs}$  and  $\delta_{ri}$  then are sufficiently large to destroy all interferences involving paths 2 and 3 (see Fig. 1). Therefore these processes only produce an unmodulated background. What remains is the interference between the processes 1 and 4 which is still possible due to the constraints for the phase deviations. The average in Eq. (2) therefore yields (for  $R = T = \frac{1}{2}$ )

$$P_{22}(\delta) = \frac{1}{4} [1 + \frac{1}{2} \cos(2\delta)]. \tag{3}$$

We thus obtain interference fringes with a visibility of 50% and a period given by the wavelength of the pump light.

The visibility of this interference can be enhanced, however, by excluding processes 2 and 3 from detection. As suggested in Refs. 5 and 6, this can be done by taking advantage of the time delay between the photons which traveled along different arms of the interferometer in these processes. Correlation measurements with adequate time resolution should allow the separation of these events. In fact, subtracting the contributions of processes 2 and 3 from the total probability, Eq. (3) is modified to

$$P_{22}(\delta) = \frac{1}{8} [1 + \cos(2\delta)], \tag{4}$$

which means that the visibility of the interference fringes is increased to 100%.

The experimental setup is shown in Fig. 2. The beam of an argon-ion laser operating at wavelength  $\lambda = 458 \text{ nm}$  serves as the pump light for the generation of parametri-

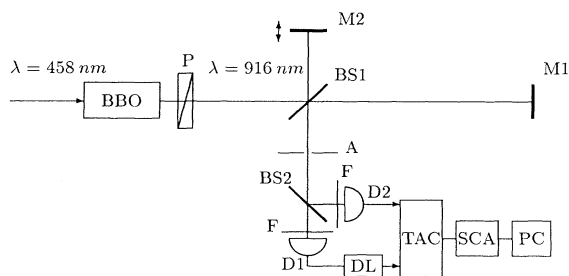


FIG. 2. Experimental setup; for details see text.

cally down-converted photon pairs in the  $\beta$ -barium-borate (BBO) crystal. By use of an intracavity etalon in the pump laser we achieve single-mode operation with 40-mW output and a spectral bandwidth of 54 MHz. The coherence length of the pump light therefore is about 5 m. Inside the crystal the pump beam subtends an angle of approximately  $25^\circ$  with the optical axis. In this way, phase matching for degenerate collinear type-I down-conversion is achieved. The pump beam is suppressed by a Glan-Thompson polarizer P and two color glass cutoff filters F. The divergence of the pump beam causes a frequency spread of the down-converted light.<sup>19</sup> The aperture A restricts the bandwidth of this light to  $\Delta\lambda \approx 100 \text{ nm}$ . The center wavelength is at  $\lambda_0 = 916 \text{ nm}$ . The photon pairs pass the Michelson interferometer composed of the semitransparent beam splitter BS1 and two highly reflecting mirrors M1 and M2. The arm lengths are set to 2 and 30 cm, respectively. Mirror M2 can be moved by a piezoelectric translation drive. The transmitted light field is detected by the “photon-pair detector”<sup>18</sup> which consists of a semitransparent beam splitter BS2 and two photon-counting avalanche photodiodes D1 and D2.

The output signals of the detectors are fed to a time-to-amplitude converter (TAC). The output of the detector which provides the stop signal for the TAC is given a bias delay of 30 ns by the unit DL. The TAC allows us to monitor the time intervals between the pulses of different detectors with a resolution of 50 ps. A single-channel analyzer (SCA) is used to set the width and position of the time interval during which incoming pulses are treated as coincident. The SCA output is fed to a PC which serves as multichannel coincidence counter and pulse-height analyzer. For recording interference fringes the channel advance of the counter is synchronized with the variation of the path difference between the interferometer arms.

A typical time-difference distribution obtained by pulse-height analysis is shown in Fig. 3. The count rates

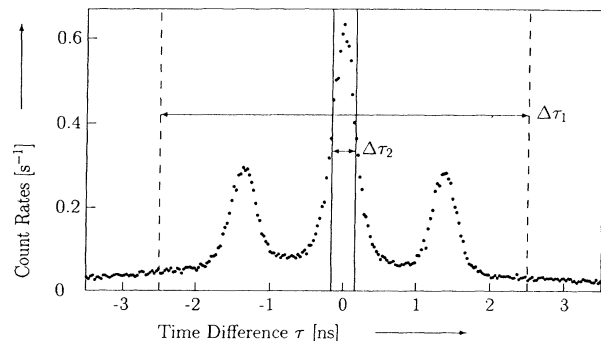


FIG. 3. Distribution of the time differences  $\tau$  in the detected photon-pair signals. The double arrows indicate time-difference windows  $\Delta\tau$  which are used for the interference experiments shown in Fig. 4.

are plotted against the time difference  $\tau$  between the output pulses of the detectors. The center peak is due to photon pairs in which both photons traveled along the same arm of the interferometer (processes 1 and 4 in Fig. 1). The registered delay for these signals is identical to the bias delay introduced for the stop-detector signal and is therefore marked as  $\tau=0$ . Two additional peaks are found at  $\tau=\pm 1.9$  ns. They belong to photon pairs which are first split and then recombined while passing the interferometer (processes 2 and 3 in Fig. 1). The measured delay is in good agreement with a time delay of  $\pm 1.87$  ns calculated from the length difference of 28 cm between the arms of the interferometer. The data points are taken as sample averages during a scan of the path difference over several wavelengths. Therefore, the relative weights of the peaks are 1:2:1 which correspond to the ratios of the mean probabilities of processes 2, 1 plus 4, and 3, respectively. The distances of the observed peaks are sufficiently large compared to their width to allow an effective separation of pairs with different time differences  $\tau$  of their photons. On the other hand, the path difference is much smaller than the coherence length of the pump laser light, such that the phase constraints are still valid.

We now set a coincidence window  $\Delta\tau$  centered at  $\tau=0$  on the time-difference distribution and record only the counts within the window while scanning the path difference between the interferometer arms. First we choose a rather broad window of  $\Delta\tau_1=5$  ns width as marked in Fig. 3 by the dashed vertical lines. The resulting interference pattern is shown in Fig. 4(a). The experimental data are represented by circles. The data are obtained by integrating the count rates over 10 s at each step of the phase scan. The rate of accidental coincidences (about  $5\text{ s}^{-1}$ ) determined by shifting the coincidence window by 5 ns has been subtracted. The figure shows interference fringes with a periodicity given by the wavelength of the pump light and a mean visibility of 46%. The solid line is a fit by the function  $P_{22}(\delta) = \frac{1}{4} [1 + 0.46 \cos(2\delta)]$ . These results compare to earlier measurements of correlation fringes<sup>5,6</sup> in Michelson interferometers.

Our electronic setup now allows us to increase the time resolution by more than 1 order of magnitude compared to previous experiments and to select only the central peak in Fig. 3. By narrowing the coincidence window to  $\Delta\tau_2=330$  ps as marked by the solid vertical lines in Fig. 3 we register [Fig. 4(b)] only those photon pairs whose photons arrive simultaneously at the two detectors. The visibility of the interference pattern increases to  $V=0.87$ . Again, accidental coincidences (about  $1\text{ s}^{-1}$ ) are subtracted. The solid line represents a fit by  $P_{22}(\delta) = \frac{1}{8} [1 + 0.87 \cos(2\delta)]$ . This visibility clearly exceeds the visibility limit of 50% which has been found in previous experiments with photon pairs in large-path-difference Michelson interferometers. The deviation

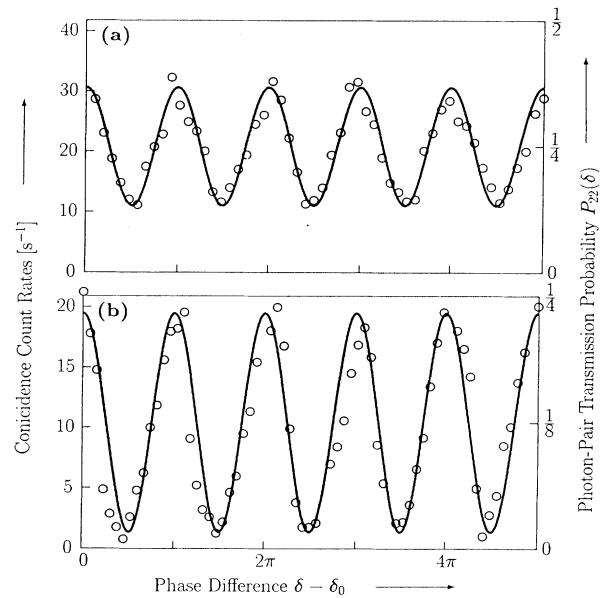


FIG. 4. Recorded fourth-order interferograms using a coincidence window width of (a)  $\Delta\tau_1=5$  ns and (b)  $\Delta\tau_2=330$  ps. The setoff  $\delta_0$  of the phase difference corresponds to a path difference of about  $6 \times 10^5 \lambda_0$ . The solid lines are fits to the experimental data as described in the text.

from the optimum value of  $V=100\%$  is due to mechanical instabilities of the interferometer, the finite size of the aperture, and a slightly different probability of the detectors to collect the photons which passed different interferometer arms.

Irrespective of the question of whether correlation interferences with visibilities below 50% can also be interpreted classically, the results presented here have no classical analogy. They are based both on the frequency constraints of the field and on the temporal correlations of the photons in the pair state. Although the frequency constraint alone explains the appearance of the interference fringes, it is the very two-particle nature of the two-photon state which allows a separation of the disturbing background intensity by the time-resolved detection scheme.

In order to perform a test of Bell's inequalities the experimental setup has to be modified to a configuration where two spatially separated interferometers are used.<sup>13,14</sup> This is the goal of a future experiment.

During the course of this work, Rarity *et al.*<sup>20</sup> as well as Ou *et al.*<sup>21</sup> demonstrated high-visibility fourth-order interferograms by a different method. They used a Mach-Zehnder interferometer in a setup where the photon pair entered the interferometer with one photon in each entrance arm. In their experiment the time-correlated photons of a pair are recombined by the semi-transparent entrance beam splitter. Because of the specific action of the beam splitter<sup>4</sup> again a selective ob-

ervation of interference between unsplit photon pairs is possible which in an ideal case would lead to visibilities of 100%. In practice, visibilities of 62% (Ref. 20) and about 75% (Ref. 21) were achieved.

Financial support by the Deutsche Forschungsgemeinschaft is gratefully acknowledged.

- <sup>1</sup>C. K. Hong, Z. Y. Ou, and L. Mandel, *Phys. Rev. Lett.* **59**, 2044 (1987).
- <sup>2</sup>R. Gosh and L. Mandel, *Phys. Rev. Lett.* **59**, 1903 (1987).
- <sup>3</sup>Z. Y. Ou and L. Mandel, *Phys. Rev. Lett.* **61**, 50 (1988); **61**, 54 (1988).
- <sup>4</sup>J. G. Rarity and P. R. Tapster, *J. Opt. Soc. Am. B* **6**, 1221 (1989).
- <sup>5</sup>P. G. Kwiat, W. A. Vareka, C. K. Hong, H. Nathel, and R. Y. Chiao, *Phys. Rev. A* **41**, 2910 (1990).
- <sup>6</sup>Z. Y. Ou, X. Y. Zou, L. J. Wang, and L. Mandel, *Phys. Rev. Lett.* **65**, 321 (1990).
- <sup>7</sup>Z. Y. Ou, E. C. Gage, B. E. Magill, and L. Mandel, *Opt. Commun.* **69**, 1 (1988).
- <sup>8</sup>L. Mandel, *Phys. Rev. A* **28**, 929 (1983).
- <sup>9</sup>Z. Y. Ou, *Phys. Rev. A* **37**, 1607 (1988).
- <sup>10</sup>R. Ghosh, C. K. Hong, Z. Y. Ou, and L. Mandel, *Phys. Rev. A* **34**, 3962 (1986).
- <sup>11</sup>M. A. Horne and A. Zelinger, in *Proceedings of the Symposium on Foundations of Modern Physics*, edited by P. Lahti and P. Mittelstaedt (World Scientific, Singapore, 1985), p. 435.
- <sup>12</sup>J. G. Rarity and P. R. Tapster, *Phys. Rev. Lett.* **64**, 2495 (1990).
- <sup>13</sup>M. Żukowsky and J. Pykacz, *Phys. Lett. A* **127**, 1 (1988).
- <sup>14</sup>J. D. Franson, *Phys. Rev. Lett.* **62**, 2205 (1989).
- <sup>15</sup>D. C. Burnham and D. L. Weinberg, *Phys. Rev. Lett.* **25**, 84 (1970).
- <sup>16</sup>S. Friberg, C. K. Hong, and L. Mandel, *Phys. Rev. Lett.* **54**, 2011 (1985).
- <sup>17</sup>E. Mohler, J. Brendel, R. Lange, and W. Martienssen, *Europhys. Lett.* **8**, 511 (1989).
- <sup>18</sup>J. Brendel, R. Lange, E. Mohler, and W. Martienssen, *Ann. Phys. (Leipzig)* (to be published).
- <sup>19</sup>C. L. Tang, in *Quantum Electronics*, edited by H. Rabin and C. L. Tang (Academic, New York, 1975).
- <sup>20</sup>J. G. Rarity, P. R. Tapster, E. Jakeman, T. Larchuk, R. A. Campos, M. C. Teich, and B. E. A. Saleh, *Phys. Rev. Lett.* **65**, 1348 (1990).
- <sup>21</sup>Z. Y. Ou, X. Y. Zou, L. J. Wang, and L. Mandel, *Phys. Rev. A* **42**, 2957 (1990).